Hyperfine Interact (2016) 237:74
DOI 10.1007/s10751-016-1299-0

Mössbauer spectra obtained using $\beta - \gamma$ coincidence method after ^{57}Mn implantation into LiH and LiD

Y. Sato[1] · Y. Kobayashi[1,2] · Y. Yamada[3] · M. K. Kubo[4] · M. Mihara[5] · T. Nagatomo[2] · W. Sato[6] · J. Miyazaki[7] · S. Tanigawa[1] · D. Natori[1] · S. Sato[8] · A. Kitagawa[8]

Abstract Highly energetic ^{57}Mn ($T_{1/2} = 1.45$ m) was generated by nuclear projectile fragmentation in a heavy-ion accelerator, and implanted into lithium hydride (LiH) and lithium deuteride (LiD) at 578 K. Mössbauer spectroscopy with $\beta - \gamma$ coincidence detection was then carried out on the ^{57}Fe obtained from β^-decay of the ^{57}Mn to study the time dependence of the site distributions and coordination environments of dilute Fe atoms implanted in the LiH and LiD. The results suggest that the Fe atoms can substitute for either the Li and H or D atoms within 100 ns. Additionally, the displacement behavior of the substitutional ^{57}Fe atoms on the lattice sites is discussed.

This article is part of the Topical Collection on *Proceedings of the International Conference on the Applications of the Mössbauer Effect (ICAME 2015), Hamburg, Germany, 13–18 September 2015*

✉ Y. Kobayashi
kyoshio@pc.uec.ac.jp

[1] Graduate School of Engineering and Science, University of Electro-Communication, Chofu, Tokyo 182-8585, Japan

[2] Nishina Center Accelerator Based Science, RIKEN, Wako, Saitama 351-0198, Japan

[3] Department of Chemistry, Tokyo University of Science, Shinjuku, Tokyo 162-8602, Japan

[4] Division of Arts Science, International Christian University, Mitaka, Tokyo 181-8585, Japan

[5] Graduate School of Science, Osaka University, Toyonaka, Osaka 560-0043, Japan

[6] Department of Chemistry, Kanazawa University, Kanazawa, Ishikawa 920-1192, Japan

[7] Department of Chemistry and Engineering, Tokyo University Agri. Technology, Koganei, Tokyo 183-0057, Japan

[8] National Institute of Radiological Sciences (NIRS), Inage, Chiba 263-8555, Japan

Published online: 02 March 2016

Keywords In-beam Mössbauer spectroscopy · ^{57}Mn ion implantation · $\beta - \gamma$ coincidence measurement · Time-resolved Mössbauer spectroscopy · Lithium hydride

1 Introduction

In-beam Mössbauer spectroscopy of solids implanted with ^{57}Mn, which decays to ^{57}Fe with a half-life of 1.45 min, enables atomic-scale investigations of the physical, chemical and magnetic properties of extremely dilute collections of Fe atoms in solids in which iron is insoluble. However, the β-rays emitted by ^{57}Mn can significantly degrade the signal-to-noise ratio for the Mössbauer spectrum when a resonance detector is used. To overcome this problem, $\beta - \gamma$ anticoincidence counting of the β-rays emitted from ^{57}Mn and the Mössbauer γ-rays has been employed to improve the quality of the Mössbauer spectrum, and can provide an adequate signal-to-noise ratio even for a very low dose of ^{57}Mn probes [1]. This method has enabled the study of the behavior of dilute and isolated Fe atoms in MgO, NaF [2], Al_2O_3 [3] and LiH [4, 5] at high temperatures and in gas matrices of Ar [6], Xe [7], and CH_4 [8] where the recoil-free fractions are low.

^{57}Mn predominantly undergoes β^-decay to the first excited state of ^{57}Fe accompanied by the emission of energetic β-rays, and this is followed by transition to the ground state with the emission of 14.4 keV Mössbauer γ-rays, as shown in Fig. 1. It is possible to measure the time-dependent Mössbauer spectrum by utilizing detection of the ^{57}Mn β-events as a start signal and detection of the subsequent 14.4 keV γ-ray emission as a stop signal. This $\beta - \gamma$ coincidence method can be used to carry out non-destructive timedependent observations of the physical and chemical states of ^{57}Fe, e.g. occupied positions, electronic states, coordination environments, and atomic diffusion, at various elapsed times after the nuclear decay. For example, our time-resolved Mössbauer spectroscopy investigation of ^{57}Fe arising from ^{57}Mn in n-type Si showed that the ^{57}Fe atoms occupy both substitutional and interstitial sites in Si within 100 ns after the β^--decay of ^{57}Mn, and that the occupancy ratio between these positions does not depend on the elapsed time after the β^--decay [9].

In this study, in-beam Mössbauer spectroscopy with $\beta - \gamma$ coincidence detection was carried out to study the time-dependent site distributions of ^{57}Fe atoms produced by the decay of ^{57}Mn implanted into LiH and LiD at high temperatures. Previously, we reported Mössbauer spectra of ^{57}Fe following ^{57}Mn implantation into LiH in the range of 11-800 K, along with *ab initio* density functional calculations [4, 5]. Above 500 K, the ^{57}Fe was predominantly trapped in Li^+ and H^- substitutional sites without creating a neighboring lattice defect due to the migration of vacancies with increasing temperature. The goal of this study was to determine the dynamic behavior of the decaying atoms prior to substitution for the matrix atoms in LiH and LiD.

2 Experimental

The experiments were carried out at the heavy-ion medical accelerator (HIMAC) at the National Institute of Radiological Science (NIRS). ^{57}Mn nuclei were produced through the nuclear projectile fragmentation of a ^{58}Fe primary beam with an energy of 500 MeV/nucleon and a ^{9}Be production target. The ^{57}Mn nuclei were separated and optimized electromagnetically by an in-flight radioisotope (RI) beam separator at HIMAC [10], and then implanted directly into LiH and LiD after passing through an energy degrader with

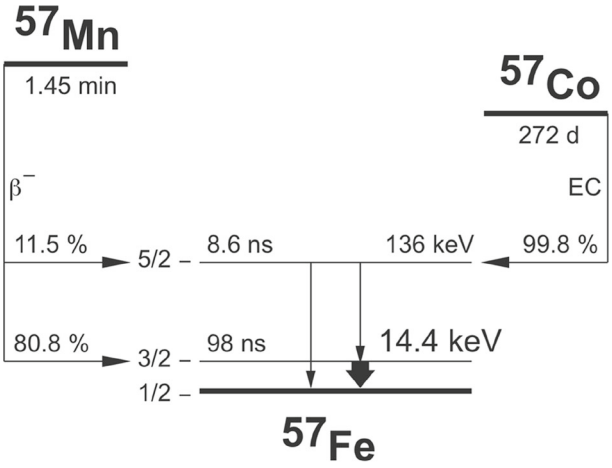

Fig. 1 Simplified scheme of ^{57}Mn decay into ^{57}Fe

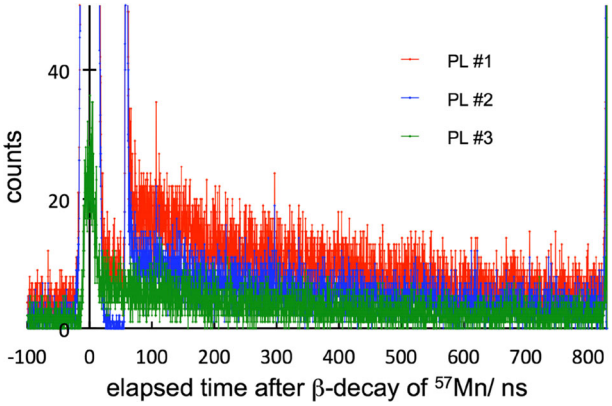

Fig. 2 Coincidence timing spectra between the β-rays detected by the scintillation counters and the Mössbauer events accumulated by the PPAC. Three plastic scintillators were placed just in front of the PPAC (PL#1), between a collimator and the sample (PL#2), and at the opposite side of the PPAC (PL#3)

the appropriate thickness. A parallel-plate avalanche counter (PPAC) installed the ^{57}Fe-enriched stainless steel as an absorber was employed to detect the internal conversion electrons emitted after resonant absorption of the Mössbauer γ-rays. Three plastic scintillation counters with photomultiplier tubes were placed around the sample for the detection of β-rays emitted from ^{57}Mn. One of them placed just in front of the PPAC also functioned as the $\beta - \gamma$ anti-coincidence counter to reduce the background caused by energetic electrons. The anti-coincidence measurement system has been described previously in detail in Ref. [1]. Using the $\beta - \gamma$ coincidence method, the Mössbauer signals obtained by the PPAC were traced back to the corresponding β-events detected by the plastic scintillators. The elapsed time between the β-events detected by the plastic scintillators and the Mössbauer γ-events registered by the PPAC was recorded on an event-by-event basis. In addition, the transducer signal corresponding to the energy shift by the Doppler velocity

of the PPAC was recorded simultaneously. All of the timing data was accumulated by a multistop time-to-digital converter (TDC) and the KODAQ program [9, 11].

The polycrystalline samples of LiH and LiD were obtained from Wako Pure Chemicals Co. (Japan) and installed on a ceramic heater in a vacuum chamber without further chemical treatment. The in-beam Mössbauer spectra of ^{57}Fe arising from the ^{57}Mn implanted in the LiH and LiD were measured at 578 K.

3 Results and discussion

Typical $\beta - \gamma$ coincidence timing spectra between the β-rays detected by each of the three scintillation counters and the γ-rays detected by the PPAC are shown in Fig. 2. The origin on the vertical axis of the plot in Fig. 2 corresponds to the emission of β-rays from ^{57}Mn. To avoid detrimental noise problems caused by β-rays, the PPAC was configured to not accumulate the Mössbauer β-events for the first few ns after the detection of β-rays. The number of γ-events decreased with the half-life of the first excited state ($t_{1/2} = 98$ ns) after the emission of β-rays.

Time-resolved Mössbauer spectra covering several regions of elapsed time after β-decay of ^{57}Mn were extracted from the timing spectra. Typical time-resolved and time-integral Mössbauer spectra of ^{57}Fe in LiH at 578 K are shown in Fig. 3. The time-integral Mössbauer spectrum was well fitted by two singlets corresponding to monovalent $^{57}Fe^{+}$ substituted for Li and H atoms respectively, which is in good agreement with our previous results [4, 5]. The time-resolved spectra at different elapsed times could be analyzed similarly using a superposition of two independent singlets. The peaks were significantly broadened for shorter elapsed times compared to those for longer elapsed times, due to the uncertainty between the duration of the observation time and the energy of the emitted γ-rays. However, we found that $^{57}Fe^{+}$ ions were incorporated into both Li and H sites within less than 100 ns following the ^{57}Mn β-decay. The appearance of two individual single lines suggests that the local environment around the Fe atoms recovered instantaneously.

^{57}Mn nuclei implanted into LiH settle at an adequate depth from the sample surface, and decay to the first excited state of ^{57}Fe which has a lifetime of 140 ns. This is followed by transition to the Fe ground state accompanied by the emission of 14.4-keV γ-rays. The γ-rays emitted from the sample generate the first excited state of ^{57}Fe nuclei contained in an absorber embedded in the PPAC via the Mössbauer effect. Then, transition from the first excited state, which has a lifetime of 140 ns, yields internal conversion electrons. Therefore, the resonance areas in the ^{57}Fe Mössbauer spectra arising from ^{57}Mn implanted into the samples correspond to the number of internal conversion electrons produced as a result of the double transition in a sample and an absorber of PPAC. Assuming that the $^{57}Fe^{+}$ ions produced after the β-decay of ^{57}Mn are simply incorporated at lattice sites in the LiH sample, the time variations of the resonance areas depend only on the lifetime of the first excited state. In this case, the number of observed internal conversion electrons was calculated using the following equation:

$$N_3 = \lambda N_1 \cdot t \cdot e^{-\lambda t}, \tag{1}$$

where N_1 is the number of ^{57}Mn nuclei implanted into LiH, N_3 is the number of internal conversion electrons detected by the PPAC, λ (s^{-1}) is the decay constant for the first excited state with the lifetime of 140 ns, and t (s) is the elapsed time after ^{57}Mn β-decay. On the other hand, when the ^{57}Mn nuclei were trapped in a well-defined rigid site of the LiH and the ^{57}Fe nuclei produced by the β-decay stayed at the same site, the observed counts should

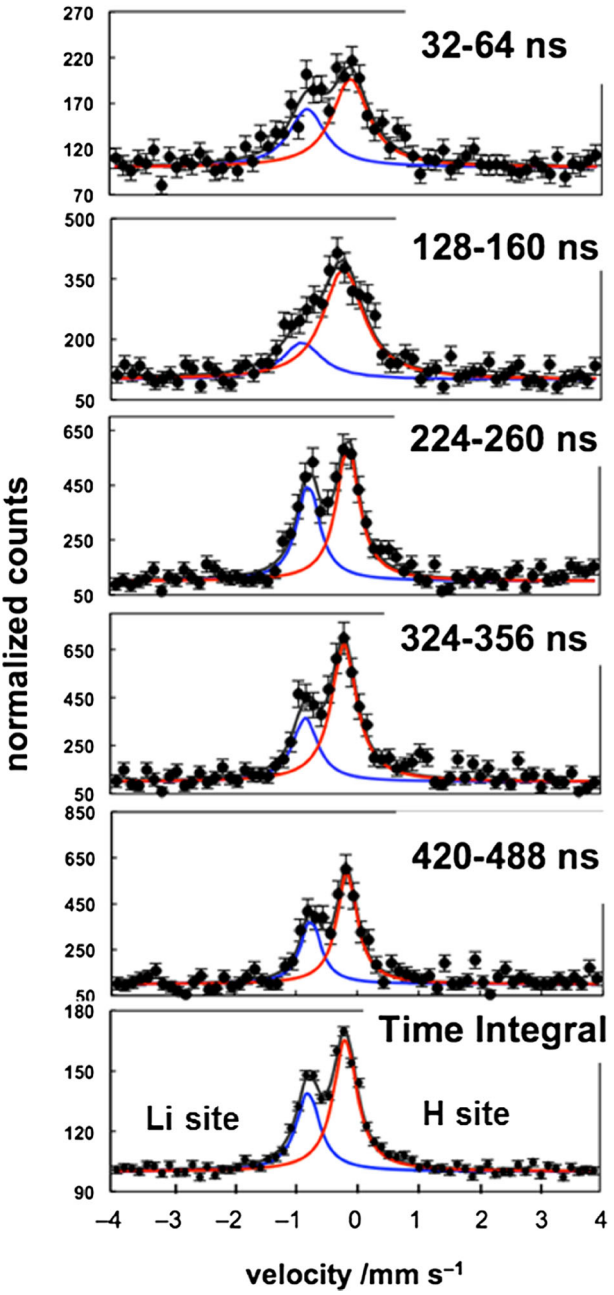

Fig. 3 Typical time-resolved ^{57}Fe Mössbauer spectra obtained with the $\beta - \gamma$ coincidence method at the different elapsed times and the time integral measurements after β-decay of ^{57}Mn implanted in LiH at 578 K. The isomer shift is relative to α-Fe at room temperature

follow the (1). But the normalized resonance area observed in our experiment, as shown in Fig. 4, did not follow the (1). This fact indicated that ^{57}Fe nuclei did not stay at the rigid site after β-decay. There was an intermediate state not observable in a Mössbauer spectrum

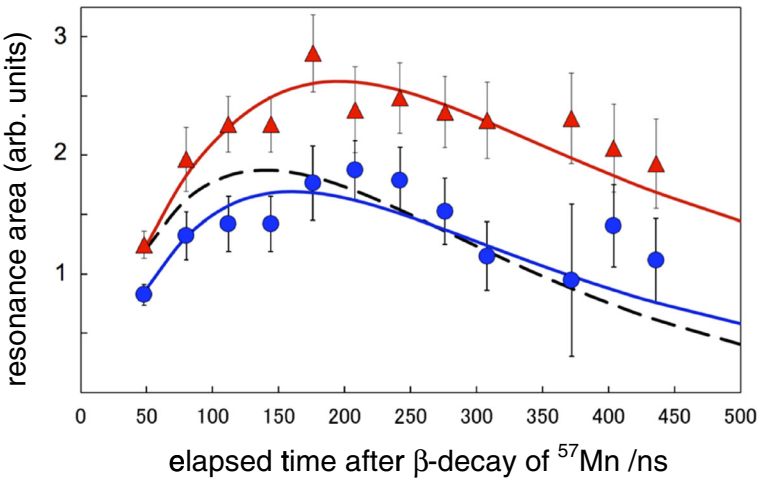

Fig. 4 Normalized resonance area as a function of the elapsed time after β-decay of ^{57}Mn in LiH at 578 K. ▲: substitutional Fe^+ ions into the H sites,●: substitutional Fe^+ ions into the Li sites. The dashed line is calculated using (1)

because of the movement of ^{57}Fe nuclei or softening of the lattice. The ^{57}Fe nuclei after β-decay move to find stable final site; the speed of displacement is defined as the displacement rate constant α (s^{-1}):

$$N_3 = \frac{\lambda N_1}{\alpha}(\alpha t + e^{-\alpha t} - 1)e^{-\lambda t} + \lambda N_2 t e^{-\lambda t}, \tag{2}$$

where N_2 is the number of ^{57}Fe atoms in a final stable site after the movement. When α is zero, the (2) is equal to the (1) because the ^{57}Fe nucleus after β-decay settles into the stable position very quickly and the amount of N_2 becomes negligible. Figure 4 shows the normalized resonance areas, which were defined by the number of internal conversion electrons, of two singlets corresponding to $^{57}Fe^+$ ions substituting either Li or H atoms as a function of the elapsed time after ^{57}Mn β-decay The dashed line on the same plot was calculated using (1), and exhibits a local maximum at an elapsed time of 140 ns, which is the lifetime of the ^{57}Fe excited state. The measured and calculated time dependence seem to differ slightly: the maximum values measured for the two components both appear at elapsed times greater than 140 ns. Using (2), the displacement rate constant α was estimated to be $(5.0\pm1.5)\times10^7$ s^{-1} ($1/\alpha = 20\pm6$ ns) and $(1.5\pm0.7)\times10^7$ s^{-1} ($1/\alpha = 70\pm30$ ns) for Li and H sites, respectively. This suggests that several tens of nanoseconds are required for the Li and H atoms in LiH to be replaced by $^{57}Fe^+$ ions. We speculate that the difference in α for the Li and H sites could depend on the charge states, electronegativities, and ionic radii of Fe, Li, H atoms; however, the details regarding the exact chemical and physical process are still under consideration.

We obtained tentative results for the time-resolved and the time-integral Mössbauer spectra in LiD at the same temperature of 578 K. These spectra had broader linewidths compared to those observed in LiH, as shown in Fig. 5. Although the statistical accuracies were not sufficient, the time-integral spectra could be fitted based on DFT calculations with four components corresponding to substitution of the $^{57}Fe^+$ ions into either the Li and D sites, and these with neighboring vacancies [5]. The time-resolved spectra were analyzed using

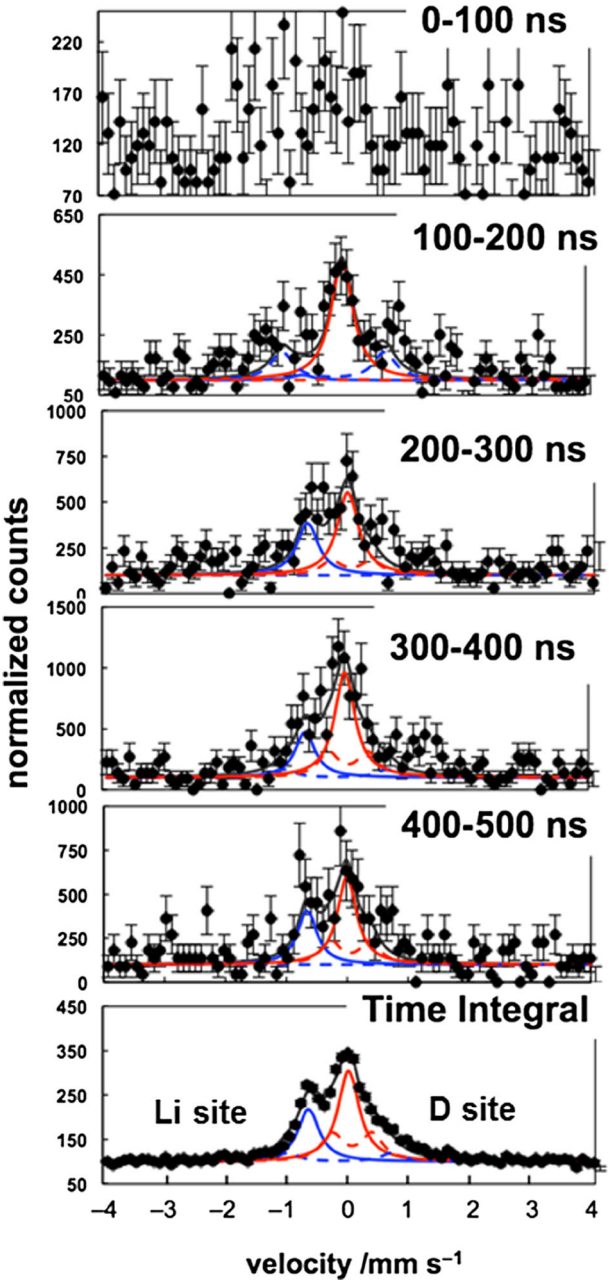

Fig. 5 Time-resolved ^{57}Fe Mössbauer spectra obtained with the $\beta - \gamma$ coincidence method at the different elapsed times, and the time integral measurements after β-decay of ^{57}Mn implanted in LiD at 578 K. The isomer shift is relative to α-Fe at room temperature

the same four components. In the case of LiD, the displacement rate constant α was tentatively obtained as (1.5±0.6) $\times$ 10^7 s^{-1} ($1/\alpha$ = 70±30 ns) and (1±0.5) $\times$ 10^7 s^{-1} ($1/\alpha$ = 100±50 ns) for the Li and D sites, respectively. Therefore, the values of α for LiD

tended to be smaller than those for LiH, indicating the presence of a kinetic isotope effect between H and D.

4 Conclusions

In-beam Mössbauer spectroscopy coupled with a $\beta - \gamma$ coincidence method was applied to study the time-dependent site distributions of ^{57}Fe atoms in LiH and LiD produced by the β-decay of ^{57}Mn implanted into the lattices at 578 K. The time-dependent Mössbauer spectra were obtained at different elapsed times following ^{57}Mn β-decay. The spectra obtained for LiH were fitted with two singlets, which were assigned to substitutional Fe^{+} ions at either the Li or H sites. The time dependence of the resonant area of the two singlets could not be explained by simple decay of the first excited state of ^{57}Fe (140 ns lifetime), which suggests that some degree of interaction occurs during the substitution of Fe atoms into Li and H sites. The values of the displacement rate constant α measured for LiH were $(5.0\pm1.5) \times 10^7$ s^{-1} for the Li site and $(1.5\pm0.7) \times 10^7$ s^{-1} for the H site.

Acknowledgments We would like to thank Dr. S. Kamiguchi of the Chemical Analysis Team in RIKEN and Associate Prof. J. Kobayashi at International Christian University for synthesizing the ^{58}Fe-enriched ferrocene that we used as an ion source for the primary beam. This work was partially supported by a Grant-in-Aid for Scientific Research (C) (KAKENHI No. 25410062) of the Japan Society for the Promotion of Science (JSPS).

References

1. Nagatomo, T., Kobayashi, Y., Kubo, M.K., Yamada, Y., Mihara, M., Sato, W., Miyazaki, J., Sato, S., Kitagawa, A.: Nucl. Inst. Meth. B **269**, 455–459 (2011)
2. Kubo, M.K., Kobayashi, Y., Yamada, Y., Mihara, M., Nagatomo, T., Sato, W., Miyazaki, J., Sato, S., Kitagawa, A.: Rev. Sci. Instrum. **85**, 02C310-3 (2014)
3. Kobayashi, Y., Nagatomo, T., Yamada, Y., Mihara, M., Sato, W., Miyazaki, J., Sato, S., Kitagawa, A., Kubo, M.K.: Hyp. Int. **198**, 173–178 (2010)
4. Nagatomo, T., Kobayashi, Y., Kubo, M.K., Yamada, Y., Mihara, M., Sato, W., Miyazaki, J., Mae, K., Sato, S., Kitagawa, A.: Hyp. Int. **204**, 125–128 (2012)
5. Miyazaki. J., Nagatomo, T., Kobayashi, Y., Kubo, M.K., Yamada, Y., Mihara, M., Sato, W., Sato, S., Kitagawa, A.: J. Radioanal. Nucl. Chem. **303**, 1155–1158 (2015)
6. Yamada, Y., Kobayashi, Y., Kubo, M.K., Mihara, M., Nagatomo, T., Sato, W., Miyazaki, J., Sato, S., Kitagawa, A.: Chem. Phys. Lett. **567**, 14–17 (2013)
7. Yamada, Y., Kobayashi, Y., Kubo, M.K., Mihara, M., Nagatomo, T., Sato, W., Miyazaki, J., Sato, S., Kitagawa, A.: Hyp. Int. **226**, 35–40 (2014)
8. Tanigawa, S., Kobayashi, Y., Mihara, M., Nagatomo, T., Yamada, Y., Kubo, M.K., Miyazaki, J., Sato, W., Sato, Y., Natori, D., Sato, S., Kitagawa, A.: Hyp. Int. submitted
9. Kobayashi, Y., Mihara, M., Nagatomo, T., Yamada, Y., Kubo, M.K., Miyazaki, J., Sato, W., Sato, S., Kitagawa, A.: Hyp. Int. **226**, 679–685 (2014)
10. Kanazawa, M., Kitagawa, A., Kouda, S., Nishino, T., Torikoshi, M., Noda, K., Murakami, T., Sato, S., Suda, M., Tomitani, T., Kanai, T., Futami, Y., Shinbo, M., Urakabe, E., Iseki, Y.: Nucl. Phys. **A746**, 393c (2004)
11. Omata, K., Fujita, Y.: IEEE Trans. Nucl. Sci. **NS39-2**, 143 (1990)